International Journal of Applied Pharmaceutics

ISSN- 0975-7058 Vol 15, Issue 6, 2023

Original Article

QUALITY BY DESIGN APPROACH FOR DEVELOPMENT AND OPTIMIZATION OF CHITOSAN-BASED FLOATING MICROSPHERES FOR TOPOTECAN HCl

PRAHLAD PRAGALLAPATI[1*], REVATHI NAGA LAKSHMI PONNURI[2], VENKATA RAMANA MURTHY KOLLAPALLI[3]

[1]University College of Pharmaceutical Sciences, Acharya Nagarjuna University, Guntur, Andhra Pradesh, India. [2]University College of Pharmaceutical Sciences and Research, Krishna University, Machilipatnam, Andhra Pradesh, India. [3]A. U. College of Pharmaceutical Sciences, Andhra University, Visakhapatnam, Andhra Pradesh, India

[*]Corresponding author: Prahlad Pragallapati; [*]Email: prahladpharma@gmail.com

Received: 14 Jul 2023, Revised and Accepted: 16 Aug 2023

ABSTRACT

Objective: To develop floating microspheres for the topotecan in order to prevent its onversion into inactive carboxylate form in intestinal pH conditions so as to improve its bioavailability.

Methods: Chitosan-based porous floating microspheres containing sodium bicarbonate by coacervation technique were developed. Quality by design approach using Box-Behnken Design was adopted to assess the influences of selected formulation variables and their importance on the quality of the finished product.

Results: The selected model was analyzed and optimized. The microspheres floated immediately without any lag time upon addition into water and remained floatable for more than 24 h^{-1}. The optimized formulation was found to have the particle size of 379.2 µm, entrapment efficiency of 76.3% and the drug release rate constant of 0.29 h i.e., the release was extended up to 16 h^{-1}.

Conclusion: The results affirmed that controlled-release porous microspheres of Topotecan with inherent floating without lag were successfully developed.

Keywords: Bio-availability, Topotecan hydrochloride, Chitosan, Floating microspheres, Quality by design

© 2023 The Authors. Published by Innovare Academic Sciences Pvt Ltd. This is an open access article under the CC BY license (https://creativecommons.org/licenses/by/4.0/)
DOI: https://dx.doi.org/10.22159/ijap.2023v15i6.48850. Journal homepage: https://innovareacademics.in/journals/index.php/ijap

INTRODUCTION

Topotecan Hydrochloride (TPT) belongs to the semi-synthetic alkaloid class derived from campothecin. The tree *Campotheca acuminata* is the source of campothecin, which acts as a chemotherapeutic alkaloid [1]. TPT acts as an anti-neoplastic agent, especially to treat retinoblastoma (eye cancer) along with other cancers like ovarian, cervical and lung cancers. Usually, cancer cells have the tendency to proliferate wildly due to a lack of control between the cell division and differentiation. Usually, anti-cancer drugs help in inhibiting the cancer cells either by blemishing the ribonucleic acid (RNA) or by blemishing the deoxyribonucleic acid (DNA), which is very much required for the cell division of cancer cells [2]. The mechanism of TPT involves encouraging the formation of fatal double-stranded DNA instead of single-stranded DNA during the S-phase of the cell cycle by hindering the required Topoisomerase-I enzyme [3].

TPT acts through the pH-dependent ring opening mechanism. Based on the surrounding pH, the lactone ring or carboxylate ring of topotecan will open and show its pharmacological activity [4]. Among both rings, the lactone ring shows anti-cancer activity by opening at an acidic pH, but the lactone ring has a rapid tendency to convert to an inactive carboxylate ring upon an increment in pH. Due to less gastric residence time, the active lactone ring will rapidly have converted to an inactive carboxylate form, reducing the bioavailability of topotecan. Along with the ring conversion, there is another obstacle to the bioavailability of TPT, i.e., the hydrophilic nature of the drug [5]. The cancer-treating drug TPT needs to act on the tumour tissues by permeating deep into them, but the negative logP value of TPT doesn't allow it to do this. So, as to improve the bioavailability of TPT, many efforts have been made with regards to formulation and have been reported in the literature. The majority of the formulations were designed as extended-release (ER) dosage forms, such as ER tablets or ER capsules, to provide continuous availability of the lactone form of TPT in the bloodstream to meet the desired therapeutic efficacy [6]. But the short residence time of 2 to 3 h for an oral dosage form in the stomach region is the disadvantage. So as to overcome the problems associated with the oral route, various researchers developed parenteral dosage forms like solid lipid nanoparticles, liposomes, and other polymeric micro- and nanoparticles to improve the bioavailability of TPT [7].

By considering the invasive methods of injectable formulations, we have decided to develop an extended-release dosage form with improved gastric residence time to provide extended drug release of TPT. In the present work, we concentrated on the development of chitosan-based floating microparticles to facilitate continuous drug release with less variability and also prevent dose dumping in GIT [8]. For the purpose of designing a formulation with the utmost quality and desired characteristics, Quality by Design (QbD) was used as a tool in the development activity [9].

By having the QbD in your hands, it is much easier to assess the outcome and the behaviour of the product with a smaller number of trials. For the development of pharmaceuticals, QbD acts as a systemic quality management system by providing the facility to study the effect of a specific range of input parameters on the outcome of the product. QbD involves the systemic development process in a stepwise manner, which begins with setting up the desired quality for the product, which can be termed the Quality target product profile (QTPP), followed by the identification of the critical quality attributes (CQAs) that represent the desired quality of the product. And critical material attributes (CMAs) related to the materials or formulation that have a direct or indirect impact on the product's quality, performance, and stability [10] also need to be identified.

In the present study, the development of chitosan-based microspheres was carried out with the target of extended drug release and absorption in the gastric region. We had developed TPT-loaded chitosan-based floating microspheres using the coacervation technique. Particle size (PS), entrapment efficiency (EE), and drug release rate constant were taken as the responses or CQAs, and the

polymer to drug ratio, concentration of polymer, concentration of coacervation aid, and the polyanionic colloid were taken as critical formulation or process parameters. Box-Behnken Design (BBD) was adopted [11] to elucidate the effect of selected variables and their importance on the quality of the finished product.

MATERIALS AND METHODS

Materials

Topotecan Hydrochloride was procured from Hetero Labs Pvt. Ltd.; chitosan, sodium tripolyphosphate and sodium alginate were bought from Sigma-Aldrich; xanthan gum was obtained from CP-Kelco and all the other materials of analytical grade were utilized.

TPT-loaded chitosan floating microspheres (TCMs)

QbD aspects of TCMs

Chitosan floating microspheres of Topotecan Hydrochloride (TCMs) were formulated using factorial design with the coacervation technique [12]. The QTPP, CQAs, and CMAs were explained below.

QTPP

The desired QTPP of the current formulation is to provide extended drug release in the acidic environment of the GIT, i.e., stomach region, to enhance the availability of the active moiety of TPT for absorption into the bloodstream, and also to make the dosage form more acceptable to the patient [13]. In addition to the aforementioned properties, the dosage form should also be smaller in size to hinder its rapid movement into the intestine region.

CQAs

Usually, the CQAs of any formulation are dependent in nature due to their variability based on the independent factors. Typically, the CQAs are termed the result of a product, which will represent its quality. In the current formulation development, PS, EE [14] and the drug release rate constant of the TCMs were selected as the responses R1, R2, and R3, respectively, and the same will be focused attentively during the entire development.

CMAs

The outcomes or the desired quality of the product will depend on the properties of either the raw material, like APIs or excipients, or the process parameters. These parameters can be stated as the critical formulation or process parameters, which are independent in nature but have a direct impact on the CQAs [15]. So, to have the best product in your hands, it is very critical to choose and optimise the CPPs. After extensive literature review, for the development of TCMs, four factors, viz., A: Polymer to drug ratio, B: Concentration of chitosan in the polymer mix (% w/w), C: Concentration of Sodium tripolyphosphate (NaTPP) (% w/v), and D: Type of polyanionic colloid (PAC), were selected as the CMAs, and the same will be optimised during the development activity.

Experimental design

To develop the formulation with the desired properties, it is very important to choose the best quality design that can evaluate the effect of all the selected numerical and categorical factors. In the current development, we had selected BBD as the experimental design, and the suggested combinations of the factors with their levels were taken as different formulations, which are shown in table 1.

Preparation of TCMs

Chitosan (40–120 mg, according to its concentration in the polymer mix and the polymer-drug ratio) was dissolved in 20 ml of 2% w/v glacial acetic acid. In this CS solution, 40 mg of TPT and 60 mg of sodium bicarbonate (a gas-generating agent) were added and subjected to vortexing on a cyclomixer for 10 min. This dispersion was labelled D1. Separately, sodium alginate (SA) or xanthan gum (XG) (40–120 mg, according to the CS concentration in the polymer mix and to the polymer-drug ratio) was added to 20 ml of water and mixed to dissolve the polymer. NaTPP (1-3% w/v) was gradually added to this. This dispersion was labelled D2. Then, D1 was slowly added dropwise into D2, which was kept under stirring at 250 rpm. The microsphere generation was observed as and when the D1 was added to the D2, but it was kept under stirring for 30 min to allow rigidization. Later, the microspheres were collected by filtration and kept for drying. The dried microspheres were stored properly until further use.

Table 1: Formulation compositions as per the BBD for developing TCMs

Formulation code assigned	Levels of factors			
	Factor A: Polymer (parts to 1 part of drug)	Factor B: CS conc. (% w/w)	Factor C: NaTPP conc. (% w/v)	Factor D: PAC type
CSS1	4.00	25.00	1.00	SA
CSS2	2.00	50.00	1.00	SA
CSS3	6.00	50.00	1.00	SA
CSS4	4.00	75.00	1.00	SA
CSS5	2.00	25.00	2.00	SA
CSS6	6.00	25.00	2.00	SA
CSS7	4.00	50.00	2.00	SA
CSS8	2.00	75.00	2.00	SA
CSS9	6.00	75.00	2.00	SA
CSS10	4.00	25.00	3.00	SA
CSS11	2.00	50.00	3.00	SA
CSS12	6.00	50.00	3.00	SA
CSS13	4.00	75.00	3.00	SA
CSX1	4.00	25.00	1.00	XG
CSX2	2.00	50.00	1.00	XG
CSX3	6.00	50.00	1.00	XG
CSX4	4.00	75.00	1.00	XG
CSX5	2.00	25.00	2.00	XG
CSX6	6.00	25.00	2.00	XG
CSX7	4.00	50.00	2.00	XG
CSX8	2.00	75.00	2.00	XG
CSX9	6.00	75.00	2.00	XG
CSX10	4.00	25.00	3.00	XG
CSX11	2.00	50.00	3.00	XG
CSX12	6.00	50.00	3.00	XG
CSX13	4.00	75.00	3.00	XG

Characterization of the TCMs

Entrapment efficiency

EE was quantified using the reverse bag dialysis method. Briefly, 2 ml of microsphere suspension was packed in a dialysis membrane and placed in 50 ml of 0.1N HCl for 8 h, and the media was analysed using UV-visible spectroscopy [16] for the quantity of free TPT in the microspheres. The amount of drug entrapped and the percentage of drug loading can be calculated using the below-mentioned formula.

$$\% \text{ Entrapment efficiency} = \frac{D_T - D_F}{D_T} x100$$

D_T-Total drug content and D_F-Free drug content

Particle size

PS was determined using microscopy techniques [17]. An optical microscope was used as an instrument to determine the particle size.

Scanning electronic microscopy (SEM)

The surface morphology of microspheres was determined using SEM. Briefly, the samples were glued to the stubs and sputtered with gold-palladium alloy at 150–200 °C [18]. The SEM was operated at 20 KV acceleration with a working distance of 12–14 mm.

Floating time

The floating time of the microspheres was evaluated along with the drug release studies in the dissolution media to know the behaviour of the formulation [19].

Swelling index

The swelling index was evaluated by soaking the microspheres in water for about 3 h. The swollen and dried weights of the microspheres were measured, and the swelling index [20] was calculated as the ratio of weight gain by the microspheres to their dry weight and expressed in percentage.

***In vitro* drug release**

This study was performed for the floating microspheres using pH 4.5 acetate buffer with 0.15% w/w Sodium lauryl sulphate as a surfactant [21]. The study was performed using a magnetic stirrer with continuous agitation.

Design validation and optimisation

The selected BBD was subjected to Design of experiments (DoE) analysis and evaluated using sequential model sum of squares analysis to choose the best regression model for studying the influence of the CMAs on the CQAs. Further Analysis of variance (ANOVA) was also applied to the selected model to determine its suitability [22]. Model optimization was also performed to have the range of input variable values in hand for desired responses.

RESULTS AND DISCUSSION

Characterization studies on the TCMs

The prepared TCMs were characterised for the percentage yield, EE, PS, and swelling index. The results are presented in table 2. The % yield of the TCMs was found to be in the range of 68.9% to 84.6%, whereas the % entrapment efficiency ranges from 42.2% to 83.2%. The particle size was determined using an optical microscope, and the results were found to be in the range of 223 µm to 568 µm. The swelling index was determined by the soaking technique, and the results were found to be in the range of 48.5% to 156.2%.

Table 2: Results of the physicochemical characterization of the TCMs (Expressed as mean±standard deviation)

Code assigned	Observed results*			
	Yield (%)	EE (%)	Particle size (µm)	Swelling index (%)
CSS1	70.5±4.1	42.2±1.9	351±23	156.2±16.4
CSS2	75.3±3.6	45.1±2.2	348±36	122.4±19.2
CSS3	68.9±4.8	53.7±4.5	426±51	144.5±21.3
CSS4	71.3±1.9	54.9±2.6	404±44	140.7±15.7
CSS5	77.1±2.7	48.3±3.7	312±27	107.5±9.4
CSS6	73.7±3.5	55.1±1.6	385±19	120.9±13.1
CSS7	75.4±6.2	57.2±2.8	374±32	125.6±16.9
CSS8	79.9±2.3	60.4±4.1	361±24	117.3±10.6
CSS9	75.6±1.5	65.8±3.5	416±38	132.5±23.1
CSS10	76.8±4.2	51.2±2.7	247±31	116.4±18.4
CSS11	78.2±3.7	57.6±3.3	223±15	98.2±13.7
CSS12	74.7±5.4	67.9±1.7	289±28	105.3±8.6
CSS13	79.4±4.8	70.5±2.9	267±30	100.9±11.9
CSX1	82.5±2.9	68.2±1.4	493±55	69.3±9.5
CSX2	80.9±6.1	64.9±0.8	372±47	58.7±10.2
CSX3	76.7±3.6	76.7±3.6	517±29	76.2±6.6
CSX4	75.4±4.4	52.6±4.2	342±18	81.5±12.4
CSX5	83.7±1.8	66.1±2.0	411±35	61.7±9.3
CSX6	79.6±4.5	81.4±4.3	568±49	82.4±12.1
CSX7	82.4±2.7	68.9±3.9	425±16	76.8±8.5
CSX8	84.1±5.3	55.6±1.2	349±38	71.9±10.3
CSX9	79.5±1.6	71.2±2.6	472±44	84.6±7.5
CSX10	83.9±4.2	79.1±4.5	451±26	51.2±6.8
CSX11	84.6±3.3	70.5±0.9	319±37	48.5±5.4
CSX12	80.2±1.9	83.2±3.4	466±41	57.1±7.9
CSX13	83.7±2.8	72.7±2.1	273±25	54.6±6.1

The swelling index was found to be highly variable, which may be due to the solubility of Chitosan [23] and Sodium alginate complex-based microspheres after 3 h. In a similar manner, the percent yield and swelling index were also influenced by the concentration and type of the PAC. The increment in sodium tripolyphosphate (NaTPP) and the increment in the cross-linking agent led to the decrease in swelling index [24]. The microspheres made of chitosan-xanthan gum also showed a lower index due to their higher density and stronger coacervation. Due to strong coacervation and a denser outer microsphere layer, the swelling nature of the microspheres gets hindered upon addition to the medium. To formulate the microspheres with the desired swelling and drug release, excess polymer needs to be added to the formulation.

Floating time was observed while performing drug release studies. Microspheres of all the formulations were found to float immediately after adding them to water, which could be due to their porous nature because of the bicarbonate. All the formulations remained floatable until the complete release of the drug. Microspheres made of CS-XG and also those microspheres cross-linked with a high amount of NaTPP exhibited floating for an extended period even after the completion of the drug release. Greater charge density and cross-linking might be responsible for this extended floating.

SEM analysis

The SEM images of the TCMs are illustrated in fig. 1. The surface was found to be slightly protruding, which may be due to the entrapment of CO2 from sodium bicarbonate during the manufacturing process. SEM images were taken for the cross-sectioned microspheres and are shown in fig. 1(b). This SEM image

illustrated many pores present inside the core of the microspheres, which might be due to gas entrapment, and thus these microspheres can be easily floatable and hence can be called floating microspheres [25].

Fig. 1: Images of Topotecan loaded chitosan based floating microspheres. (a) Photographic image; (b) SEM image of the cross-sectioned microspheres indicating inner pores as cavities (at 65x magnification)

Table 3: ANOVA test results for the quadratic model for the particle size (R1)

Source	Sum of squares	Degrees of freedom	Mean sum of squares	F value	p-Value	Inference[a]
Model	$1.78x10^5$	13	13672.37	33.21	<0.0001	Significant
A-Polymer	44521.00	1	44521.00	108.14	<0.0001	Significant
B-CS conc.	6972.25	1	6972.25	16.94	0.0014	Significant
C-NaTPP conc.	32220.25	1	32220.25	78.26	<0.0001	Significant
D-PAC	42808.65	1	42808.65	103.98	<0.0001	Significant
AB	338.00	1	338.00	0.82	0.3827	
AC	12.50	1	12.50	0.030	0.8646	
AD	5625.00	1	5625.00	13.66	0.0031	Significant
BC	450.00	1	450.00	1.09	0.3164	
BD	25600.00	1	25600.00	62.18	<0.0001	Significant
CD	5184.00	1	5184.00	12.59	0.0040	Significant
A^2	787.50	1	787.50	1.91	0.1918	
B^2	52.07	1	52.07	0.13	0.7283	
C^2	8305.79	1	8305.79	20.17	0.0007	Significant
Residual	4940.35	12	411.70			
Cor Total	$1.83x10^5$	25				

Note: [a]-p-Value less than 0.05 indicates model terms are significant

DoE analysis of the particle size (R1)

Particle size results are presented in table 2 and analysed using the sequential model sum of squares to identify the ideal regression model between the selected variables and response. After the analysis, it was found that the Quadratic model was the suggested model to elaborate on the influence of the CMAs on the R1. To evaluate the significance of variables, ANOVA was also applied to the suggested quadratic model to find the suitability of the design [26]. The analysis results are shown in table 3 and fig. 2. From the analytical results, it was shown that the selected model was significant and could be progressed to further optimisation. The regression equation was also calculated for the particle size, and the formula is shown below [27].

Regression equation for the R1

$$\text{Particle Size} = +399.50 + 52.75 * A - 20.87 * B - 44.88 * C + 40.58 * D - 6.50 * AB - 1.25 * AC + 18.75 * AD - 7.50 * BC - 40.00 * BD + 18.00 * CD + 13.12 * A^2 - 3.37 * B^2 - 42.63 * C^2$$

The factors were found to have a quadratic effect on the particle size of TCSs (fig. 2). Upon an increase in the polymer content (Factor A), the size was found to increase. This result was obvious, as this could be due to greater viscosity and, hence, minimal size reduction of the coacervate at higher polymer content. By increasing the CS concentration (Factor B), the size was found to be enlarged in the case of CS-SA microspheres and diminished in the case of CS-XG microspheres. This might be because of the higher molecular weights of the colloids. The molecular weight of CS is greater than that of SA and less than that of XG. Higher molecular weight and, hence, higher viscosity would result in increased particle size. By increasing the NaTPP concentration (Factor C), the size was decreased. This could be because of the strong cross-linking, which made the coacervate denser and, hence, reduced the size. The type of PAC (Factor D) also influenced the particle size. The microspheres made of CS-XG exhibited greater size than those made of CS-SA. Again, this could be because of the greater viscosity of the XG than that of the SA.

DoE analysis of the entrapment efficiency (R2)

The EE results are given in table 2 and analysed using the sequential model sum of squares to identify the ideal regression model between the selected variables and response. After the analysis, it was found that the 2-factorial interaction (2FI) model was suggested to elaborate on the influence of the CMAs on the R2 [28]. To evaluate the significance of variables, ANOVA was also applied to the suggested model to determine the suitability of the design. The analysis results are shown in table 4 and fig. 3. From the ANOVA results, it was also evident that the model was significant and could be navigated to develop design space.

Regression equation for the R2

$$EE = +63.12 + 5.41 * A + 0.76 * B + 5.90 * C + 6.97 * D - 0.14 * AB + 0.33 * AC + 1.52 * AD + 1.98 * BC - 6.09 * BD - 0.51 * CD$$

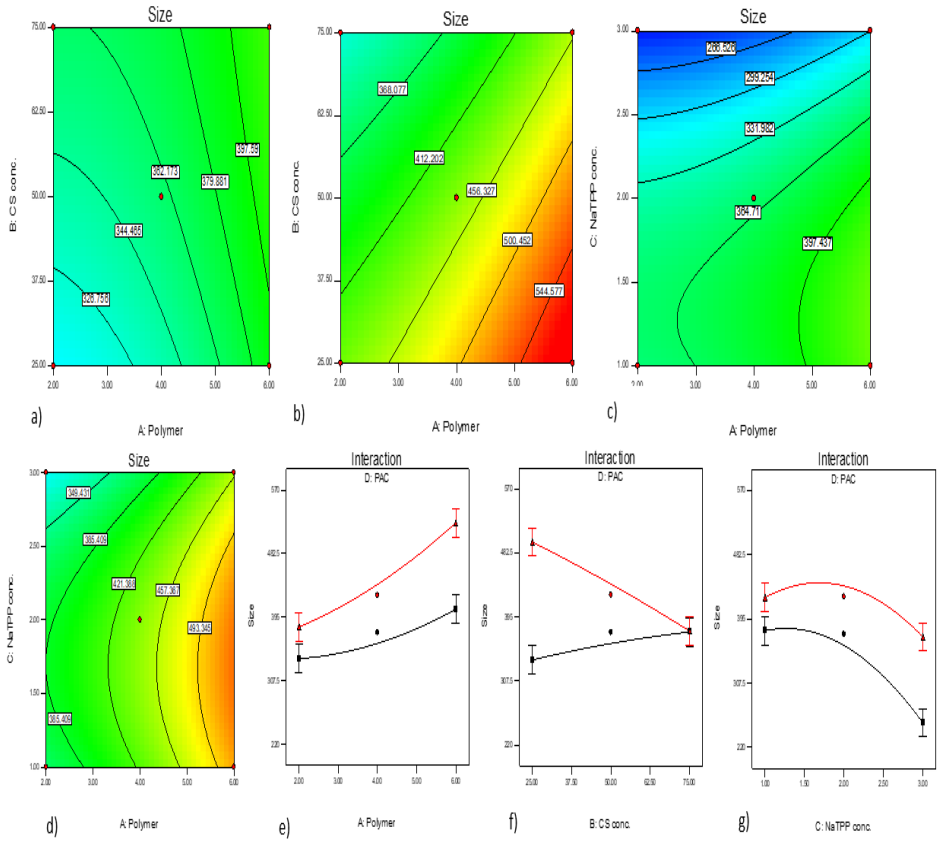

Fig. 2: Contour plots showing the effect of the factors a) A and B on the R1 in case of SA as the PAC; b) A and B on the R1 in case of XG as the PAC; c) A and C on the R1 in case of SA as the PAC; d) A and C on the PS in case of XG as the PAC. Interaction plots showing the effect of the interaction e) AD on the R1; f) BD on the R1; g) CD on the R1

Table 4: ANOVA test results for the 2FI model for the EE (R2)

Source	Sum of squares	Degrees of freedom	Mean sum of squares	F value	p-Value	Inference[a]
Model	2964.03	10	296.40	26.91	<0.0001	Significant
A-Polymer	467.64	1	467.64	42.45	<0.0001	Significant
B-CS conc.	9.15	1	9.15	0.83	0.3765	
C-NaTPP conc.	556.96	1	556.96	50.56	<0.0001	Significant
D-PAC	1262.82	1	1262.82	114.63	<0.0001	Significant
AB	0.15	1	0.15	0.014	0.9083	
AC	0.84	1	0.84	0.077	0.7856	
AD	36.91	1	36.91	3.35	0.0871	
BC	31.20	1	31.20	2.83	0.1131	
BD	594.14	1	594.14	53.93	<0.0001	Significant
CD	4.20	1	4.20	0.38	0.5461	
Residual	165.25	15	11.02			
Cor Total	3129.27	25				

Note: [a]-p-Value less than 0.05 indicates model terms are significant.

From the two-factorial design, it was found that entrapment efficiency was improved upon increasing the polymer content (Factor-A). The reason behind the increment in entrapment efficiency might be due to the increased binding nature of the polymer. With an increment in polymer content, the binding nature can also be improved, which in turn improves the entrapment efficiency of the drug [29].

The increase in the level of factor B led to an increment in EE in the case of CS-SA microspheres, whereas the same was found to be decreased in the case of CS-XG microspheres. The molecular weights and binding natures of the colloids might be the reason behind the vice-versa behaviour of the entrapment efficiency. By having a higher molecular weight of chitosan than sodium alginate, the CS-SA microspheres exhibit increased entrapment efficiency due to their higher viscosity and higher binding nature with the TPT. Whereas the molecular weight of xanthan gum was found to be higher than that of chitosan, which led to a decrease in entrapment efficiency due to a weaker interaction between the TPT and the polymer. The effect of NaTPP concentration showed a positive effect on the entrapment efficiency, which could be due to the strong cross-linking, which in turn made the coacervation denser and prevented the leakage of the entrapped drug.

DoE analysis of the drug release rate constant (R3)

The drug release studies were performed for the formulated microspheres in pH 4.5 acetate buffer with 0.15% SLS, and the drug release profiles are presented in fig. 4. Results for the drug release rate constant are given in table 5, and the data was analysed using

the sequential model sum of squares to identify the ideal regression model between the selected variables and response. After the analysis, it was found that the 2FI model was suggested to elaborate on the influence of the CMAs on the R3. To evaluate the significance of variables, ANOVA was also applied to the suggested model to determine its suitability. The analysis results are shown in table 6.

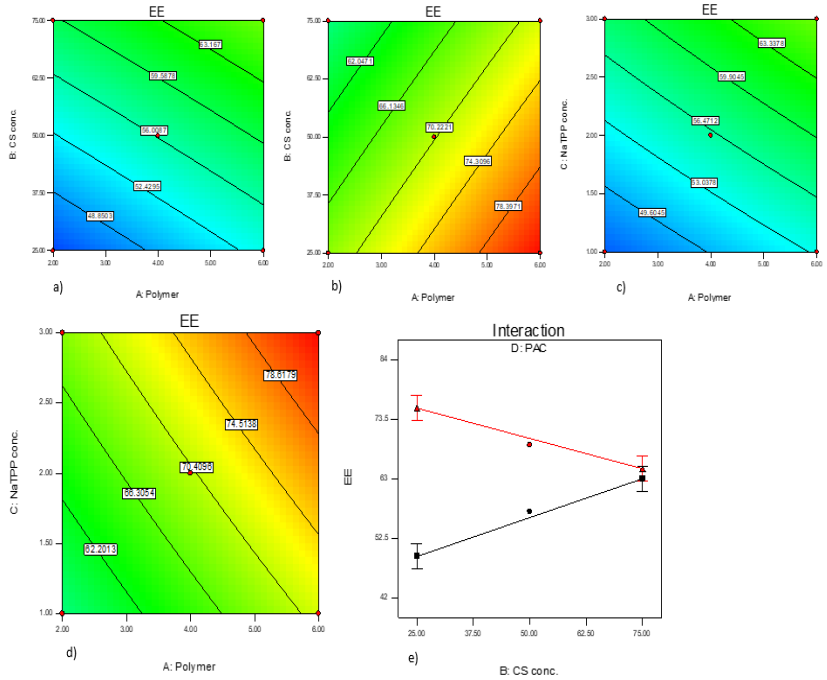

Fig. 3: Contour plots illustrating the effects of the factors a) A and B on the EE in case of SA as the PAC; b) A and B on the EE in case of XG as the PAC; c) A and C on the EE in case of SA as the PAC; d) A and C on the EE in case of XG as the PAC; e) Interaction plot for the effect of BD on the EE

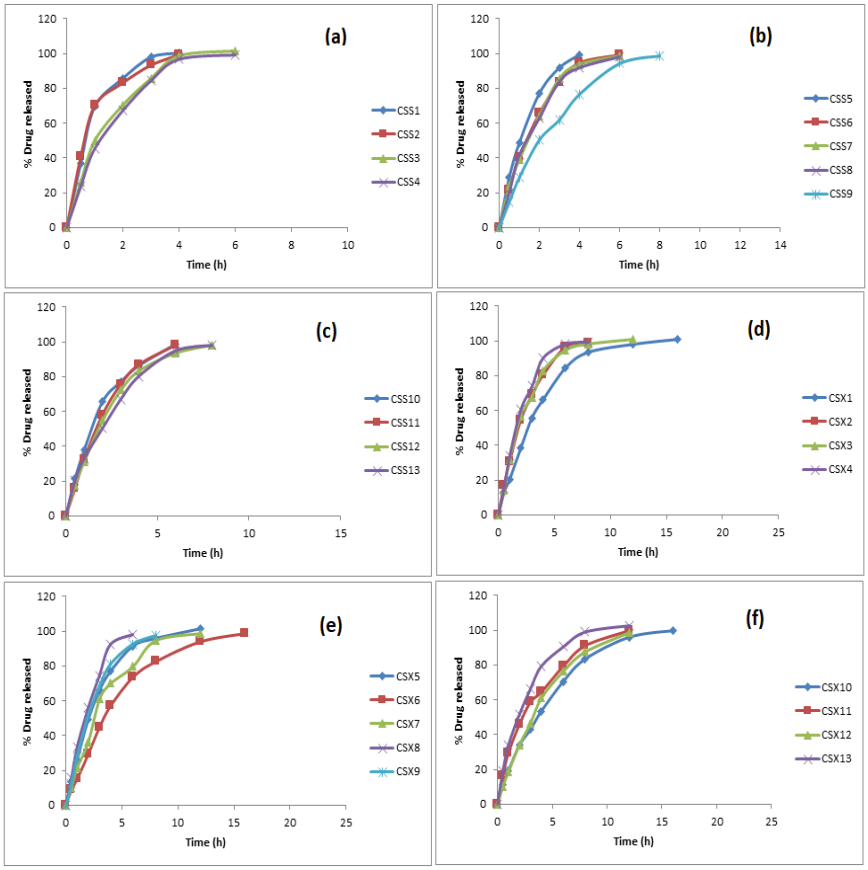

Fig. 4: Drug release profiles of TCMs of formulations (a) CSS1–CSS4; (b) CSS5–CSS9; (c) CSS10–CSS13; (d) CSX1–CSX4; (e) CSX5–CSX9; (f) CSX10–CSX13

Table 5: Drug release kinetics data from the TCMs

Code	Correlation coefficients		Drug release rate constant (k, h^{-1})	Higuchi's correlation coefficient	Korsemeyer–Peppas '*n*' value
	Zero-order	First order			
CSS1	0.603	0.968	1.19	0.951	0.465
CSS2	0.546	0.938	1.12	0.946	0.406
CSS3	0.641	0.883	0.87	0.97	0.547
CSS4	0.685	0.967	0.79	0.966	0.589
CSS5	0.833	0.932	0.98	0.986	0.607
CSS6	0.737	0.975	0.72	0.966	0.639
CSS7	0.73	0.988	0.67	0.965	0.611
CSS8	0.74	0.991	0.63	0.96	0.645
CSS9	0.819	0.945	0.49	0.974	0.696
CSS10	0.764	0.945	0.61	0.979	0.626
CSS11	0.844	0.959	0.57	0.965	0.748
CSS12	0.717	0.991	0.48	0.96	0.644
CSS13	0.748	0.982	0.46	0.982	0.592
CSX1	0.552	0.992	0.32	0.938	0.630
CSX2	0.754	0.968	0.52	0.972	0.655
CSX3	0.465	0.989	0.47	0.922	0.617
CSX4	0.677	0.955	0.61	0.949	0.679
CSX5	0.577	0.994	0.39	0.944	0.648
CSX6	0.732	0.981	0.25	0.957	0.734
CSX7	0.711	0.975	0.35	0.95	0.738
CSX8	0.85	0.952	0.62	0.957	0.757
CSX9	0.775	0.993	0.43	0.859	0.748
CSX10	0.736	0.949	0.28	0.974	0.652
CSX11	0.638	0.871	0.41	0.983	0.565
CSX12	0.819	0.94	0.31	0.965	0.737
CSX13	0.495	0.931	0.48	0.952	0.534

The ANOVA test results indicated that the model was found to be significant, which indicated the suitability of the design for the selected factors and the obtained response results. Altogether, the diagnostic results indicated that this model was significant and could be navigated to develop design space.

Regression equation for the R3

$$k = +0.58 - 0.076 * A - 0.014 * B - 0.14 * C - 0.16 * D + 0.009 * AB + 0.014 * AC + 0.016 * AD + 0.020 * BC + 0.13 * BD + 0.088 * CD$$

Table 6: ANOVA results for the quadratic model for the drug release rate constant (R3)

Source	Sum of squares	Degree of freedom	Mean sum of squares	F value	p-Value	Inference*
Model	1.47	10	0.15	45.33	<0.0001	Significant
A-Polymer	0.093	1	0.093	28.60	<0.0001	Significant
B-CS conc.	$3.306x10^{-3}$	1	$3.306x10^{-3}$	1.02	0.3294	
C-NaTPP conc.	0.33	1	0.33	100.75	<0.0001	Significant
D-PAC	0.66	1	0.66	202.64	<0.0001	Significant
AB	$6.125x10^{-4}$	1	$6.125x10^{-4}$	0.19	0.6705	
AC	$1.513x10^{-3}$	1	$1.513x10^{-3}$	0.46	0.5057	
AD	$4.225x10^{-3}$	1	$4.225x10^{-3}$	1.30	0.2723	
BC	$3.200x10^{-3}$	1	$3.200x10^{-3}$	0.98	0.3370	
BD	0.26	1	0.26	79.17	<0.0001	Significant
CD	0.12	1	0.12	38.20	<0.0001	Significant
Residual	0.049	15	$3.253x10^{-3}$			
Cor Total	1.52	25				

*p-Value less than 0.05 indicates model terms are significant

The influences of the CMAs on the R3 were illustrated in fig. 5. Upon an increase in the polymer content (Factor A), the rate constant was observed to decline. This result might be due to strong binding of the drug and increased diffusion path length for drug release, hence decreased drug release at higher polymer content [30]. The influence of Factor B on the R3 was inversely correlated with that of the release rate constant. Upon an increase in the CS concentration (Factor B), the rate constant was found to decrease in the case of CS-SA microspheres and increase in the case of CS-XG microspheres. This might be because of the molecular weights and the resultant gel matrices of the colloids. The molecular weight of CS is greater than that of SA and less than that of XG. Upon an increase in the CS concentration, the gel matrix in the case of CS-SA microspheres could become more complex. Whereas, in the case of CS-XG microspheres, the increase in CS concentration (and so a lesser XG concentration) could result in decreased gel matrix complexity. A higher molecular weight of the polymer, and hence the resultant strong gel matrix, could prolong the drug release [31]. Upon increasing the level of Factor C, the response R3 was observed to decline. This could be because of the strong cross-linking, which made the gel matrix denser, and hence the drug release was prolonged and the rate constant decreased. The type of PAC (Factor D) also influenced the rate constant. The microspheres made of CS-XG exhibited lower rate constants than those made of CS-SA. Again, this could be because of the stronger gel matrix of the XG than that of the SA, which could slow and prolong the drug release.

Formulation optimization

The formulation was optimised to find the best possible amalgamation(s) of the chosen variables to accomplish the

required results of the selected responses. The QTPP of the design is to achieve chitosan-based floating microspheres with greater entrapment efficiency and extended drug release in gastric conditions [32]. So as to achieve the target, optimisation was performed on the model with the target of minimum size, maximum EE, and minimum release rate constant (table 7). The resulted overlay is presented in fig. 6. The design space shown by the yellow colour region indicates the area inside which the combination of the CMAs can provide the floating TCMs with the desired responses.

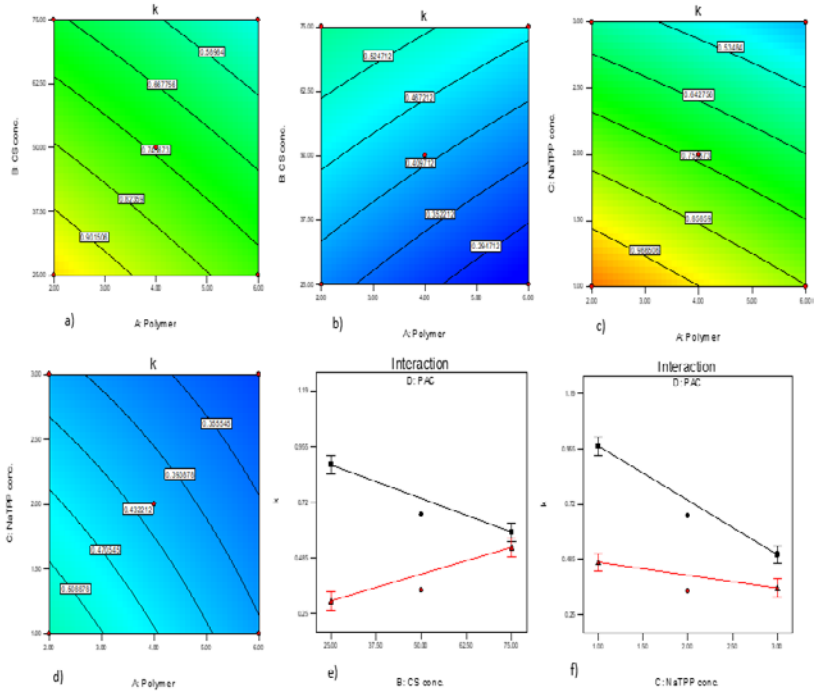

Fig. 5: Contour plots showing the effects of the factors a) A and B on the R3 in case of SA as the PAC; b) A and B on the R3 in case of XG as the PAC; c) A and C on the R3 in case of SA as the PAC; d) A and C on the R3 in case of XG as the PAC. Interaction plots illustrating the effect of e) BD interaction on the R3; f) CD interaction on the R3

Table 7: Constraints for desirability criteria

Name	Goal
A: Polymer	Is in range
B: CS conc.	Is in range
C: NaTPP conc.	Is in range
D: PAC	Is in range
R1: Size	Minimize (with the maximum limit of 400 µm)
R2: EE	Maximize (with the minimum limit of 70%)
R3: *k*	Minimize (with the maximum limit of 0.31 h^{-1})

One such formulation, identified by point prediction by the software along with the predicted responses, is mentioned in table 8. A fresh floating TCM formulation was prepared at the suggested combination and tested for quality control tests, including particle size, EE, and drug release.

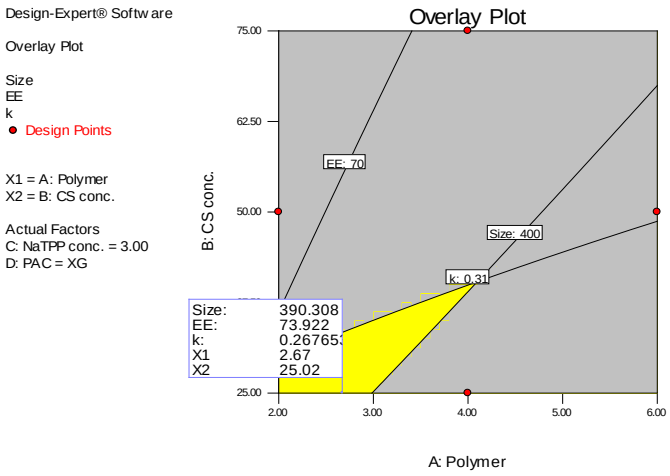

Fig. 6: Overlay plot indicating the design space

Table 8: Predicted and observed values of the responses of the optimized TCMs

Combination of the factors' levels	Responses	Predicted values	95% CI low	95% CI high	Observed values
A: Polymer (2.67 parts)	R1: Particle size (µm)	390.32	353.58	427.06	379.2
B: CS conc. (25.02 % w/w)	R2: EE (%)	73.92	68.37	79.48	76.3
C: NaTPP conc. (3.00 % w/v)	R3: k (h^{-1})	0.27	0.17	0.36	0.29
D: PAC (XG)					

The observed results were correlated (with 95% confidence intervals (CI)) with those predicted by the design, and hence this combination was considered the optimum formulation of the chitosan-based microspheres of TPT.

CONCLUSION

The Topotecan HCL-loaded floating microspheres were prepared using the coacervation technique using the StatEase software as a quality-maintaining tool. The Box-Bhenken design was used as a quality tool to design the experiments with the selected dependent and independent variables. Further, the significance of the model for each response was analysed by the ANOVA. The CMAs were optimised with the help of desirability criteria to have low particle size, high EE, and a lower dissolution rate constant. Upon construction of the overlay plot, the model suggested a formula that provided the predicted particle size of 390.32 µm, the % entrapment efficiency of 73.92%, and the dissolution rate constant of 0.27 h^{-1} against the observed values of 379.2 µm, 76.3%, and 0.29 h, respectively. The obtained values were in correlation with the predicted values by the design, with a 95% confidence interval. Hence, it is clear that the selected dependent and independent factors are significant in the development of floating microspheres and also that the selected design was proved to be valid with the application of ANOVA and by providing the optimised formula with desirable responses. Upon correlation between the design predicted values and observed values, it was clear that the aim of developing the TPT-loaded chitosan-based floating microspheres was fulfilled.

ACKNOWLEDGEMENT

The authors are thankful to the Acharya Nagarjuna University, Guntur for providing the opportunity to carry out this research work.

ABBREVIATIONS

ANOVA: Analysis of Variance; BBD: Box-Behnken Design; CI: Confidence Intervals; CQAs: Critical Quality Attributes; CMAs: Critical Material Attributes; DoE: Design of Experiments; EE: Entrapment Efficiency; ER: Extended Release; NaTPP: Sodium Tripolyphosphate; PAC: Poly Anionic Colloid; PS: Particle Size; QbD: Quality by Design; QTPP: Quality Target Product Profile; TCMs: SA: Sodium Alginate; SEM: Scanning Electronic Microscopy; TPT loaded Chitosan floating Microspheres; TPT: Topotecan hydrochloride; XG: Xanthan Gum.

FUNDING

The authors did not receive funding in any manner to carry out the work presented in this manuscript.

AUTHORS CONTRIBUTIONS

PP has executed the work, analysed and documented the results, and developed the manuscript; VRMK has designed the work plan and supervised the execution and results analysis; RNLP has involved in results analysis, manuscript writing and grammatical corrections.

CONFLICTS OF INTERESTS

The authors declaring that there are nor conflicts of interests regarding this work.

REFERENCES

1. Swamy MK, Nath S, Paul S, Jha NK, Purushotham B, Rohit KC. Biotechnology of camptothecin production in *Nothapodytes nimmoniana*, *Ophiorrhiza* sp. and *Camptotheca acuminata*. Appl Microbiol Biotechnol. 2021 Dec;105(24):9089-102. doi: 10.1007/s00253-021-11700-5, PMID 34850279.
2. Laham Karam N, Pinto GP, Poso A, Kokkonen P. Transcription and translation inhibitors in cancer treatment. Front Chem. 2020 Apr 21;8:276. doi: 10.3389/fchem.2020.00276, PMID 32373584.
3. Oliveira EA, Chauhan J, Silva JRD, Carvalho LADC, Dias D, Carvalho DG. TOP1 modulation during melanoma progression and in adaptative resistance to BRAF and MEK inhibitors. Pharmacol Res. 2021;173:105911. doi: 10.1016/j.phrs.2021.105911. PMID 34560251.
4. From the American Association of Neurological Surgeons (AANS), American Society of Neuroradiology (ASNR), Cardiovascular and Interventional Radiology Society of Europe (CIRSE), Canadian Interventional Radiology Association (CIRA), Congress of Neurological Surgeons (CNS), European Society of Minimally Invasive Neurological Therapy (ESMINT), European Society of Neuroradiology (ESNR), European Stroke Organization (ESO), Society for Cardiovascular Angiography and Interventions (SCAI), Society of Interventional Radiology (SIR), Society of NeuroInterventional Surgery (SNIS), and World Stroke Organization (WSO), Sacks D, Baxter B, Campbell BCV, Carpenter JS, Cognard C. Multisociety consensus quality improvement revised consensus statement for endovascular therapy of acute ischemic stroke. Int J Stroke. 2018 Aug;13(6):612-32. doi: 10.1177/1747493018778713, PMID 29786478.
5. Mills H, Acquah R, Tang N, Cheung L, Klenk S, Glassen R. A critical scrutiny on liposomal nanoparticles drug carriers as modelled by topotecan encapsulation and release in treating cancer. Evid Based Complement Alternat Med. 2022 Aug 9;2022:7702512. doi: 10.1155/2022/7702512, PMID 35983007.
6. Xing R, Mustapha O, Ali T, Rehman M, Zaidi SS, Baseer A. Development, characterization, and evaluation of SLN-loaded thermoresponsive hydrogel system of topotecan as biological macromolecule for colorectal delivery. BioMed Res Int. 2021 Jul 3;2021:9968602. doi: 10.1155/2021/9968602, PMID 34285920.
7. Bibi M, ud Din F, Anwar Y, Alkenani NA, Zari AT, Mukhtiar M, Zeid IMA, Althunaiti EH, Nazish H, Zeb A, Ullah I. Cilostazol-loaded solid lipid nanoparticles: Bioavailability and safety evaluation in an animal model. J Drug Deliv Sci. Technol. 2022 Aug 1;74:103581. doi: 10.1016/j. jddst.2022.103581.
8. Krishna KA, Srivastava R. *In vitro in vivo* studies on floating microspheres for gastroretentive drug delivery system: a review. Asian J Pharm Clin Res. 2021 Jan 7;14(1):13-26. doi: 10.22159/ajpcr.2021.v14i1.39183.
9. Hua Y, Su Y, Zhang H, Liu N, Wang Z, Gao X. Poly(lactic-co-glycolic acid) microsphere production based on quality by design: a review. Drug Deliv. 2021 Jan 1;28(1):1342-55. doi: 10.1080/10717544.2021.1943056, PMID 34180769.
10. Rapalli VK, Banerjee S, Khan S, Jha PN, Gupta G, Dua K. QbD-driven formulation development and evaluation of topical hydrogel containing ketoconazole loaded cubosomes. Mater Sci Eng C Mater Biol Appl. 2021 Feb 1;119:111548. doi: 10.1016/j.msec.2020.111548. PMID 33321612.
11. Srikar G, Rani AP. Tenofovir loaded poly (lactide-co-glycolide) nanocapsules: formulation optimization by desirability functions approach. Ind J Pharm Educ Res. 2020 Apr 1;54(2S):s230-40. doi: 10.5530/ijper.54.2s.79.
12. Tavares L, Santos L, Norena CPZ. Microencapsulation of organosulfur compounds from garlic oil using β-cyclodextrin and complex of soy protein isolate and chitosan as wall materials: a comparative study. Powder Technol. 2021 Sep 1;390:103-11. doi: 10.1016/j.powtec.2021.05.080.

13. Srikar G, Shanthi D, Ramesh J, Kalyani V, Nagamma I. Floating microspheres: a prevailing trend in the development of gastroretentive drug delivery system. Asian J Pharm. 2018 Nov 11;12(04):235-42. doi: 10.22377ajp.v12i04.2831.
14. Dewangan HK, Sharma A, Mishra A, Singour P. Mucoadhesive microspheres of atorvastatin calcium: rational design, evaluation and enhancement of bioavailability. Indian J Pharm Educ Res. 2021 Nov;55(3S):S733-41. doi: 10.5530/ijper.55.3s.180.
15. Grandhi S, Rani AP, Pathuri R. Voriconazole solid lipid nanoparticles: optimization of formulation and process parameters. Res J Pharm Technol. 2018 Jul;11(7):2829-35. doi: 10.5958/0974-360X.2018.00522.X.
16. Bairam R, Kumar Tatapudi H, Gajji N, Harun Rasheed S. UV spectrophotometric and HPLC method for quantification of ticagrelor in bulk and tablet dosage form. Asian J Pharm Anal. 2022:159-65. doi: 10.52711/2231-5675.2022.00027.
17. Yang B, Xu L, Liu Y, Liu B, Zhang M. Preparation of monodisperse polystyrene microspheres with different functional groups using soap-free emulsion polymerization. Colloid Polym Sci. 2021 Jul;299(7):1095-102. doi: 10.1007/s00396-021-04830-9.
18. Mohammadpour F, Kamali H, Hadizadeh F, Bagheri M, Shiadeh SNR, Nazari A. The PLGA microspheres synthesized by a thermosensitive hydrogel emulsifier for sustained release of risperidone. J Pharm Innov. 2022 Apr 5;17(3):712-24. doi: 10.1007/s12247-021-09544-7.
19. Bhise M, Shukla K, Jain S, Bhajipale N, Sudke S, Burakle P. Development and evaluation of floating microspheres of anticonvulsant drug by 3^2 full factorial design. Turk J Pharm Sci. 2022 Oct;19(5):595-602. doi: 10.4274/tjps.galenos.2021.53050. PMID 36317946.
20. Frenț OD, Duteanu N, Teusdea AC, Ciocan S, Vicaș L, Jurca T. Preparation and characterization of chitosan-alginate microspheres loaded with quercetin. Polymers. 2022 Jan 26;14(3):490. doi: 10.3390/polym14030490, PMID 35160478.
21. Aldawsari HM, Naveen NR, Alhakamy NA, Goudanavar PS, Rao GK, Budha RR. Compression-coated pulsatile chronomodulated therapeutic system: QbD assisted optimization. Drug Deliv. 2022 Dec 31;29(1):2258-68. doi: 10.1080/10717544.2022.2094500, PMID 35838522.
22. Sharma K, Porat ZE, Gedanken A. Designing natural polymer-based capsules and spheres for biomedical applications-a review. Polymers. 2021 Dec 9;13(24):4307. doi: 10.3390/polym13244307, PMID 34960858.
23. Sagar S, Pramodini GN. Formulation development and characterization of lafutidine raft system. Int J Pharm Pharm Sci. 2023 Apr 1;15(4):8-15. doi: 10.22159/ijpps.2023v15i4.47068.
24. Pathak S, Vyas SP, Pandey A. Development, characterization and *in vitro* release kinetic studies of ibandronate loaded chitosan nanoparticles for effective management of osteoporosis. Int J App Pharm. 2021 Nov 7;13(6):120-5. doi: 10.22159/ijap.2021v13i6.42697.
25. Pączkowski P, Gawdzik B. Studies on preparation, characterization and application of porous functionalized glycidyl methacrylate-based microspheres. Materials (Basel). 2021 Mar 16;14(6):1438. doi: 10.3390/ma14061438, PMID 33809475.
26. Srikar G, Avula P, Annapurna S, Boola M. Development of extended release matrix tablets of felodipine through solid dispersions for better drug release profile by a 3^2 factorial design. Indian J Pharm Educ Res. 2016 Apr 1;50(2):S89-99. doi: 10.5530/ijper.50.2.23.
27. Lebouachera SEI, Ghriga MA, Salha GB, Hadri HE, Hasanzadeh M, Drouiche N. Optimization of zero-shear viscosity for HPAM-polystyrene microspheres formulations through experimental design approach. J Polym Res. 2021 Apr;28(4):135. doi: 10.1007/s10965-021-02473-6.
28. Noureen S, Noreen S, Ghumman SA, Batool F, Hameed H, Hasan S. *Prunus armeniaca* gum-alginate polymeric microspheres to enhance the bioavailability of tramadol hydrochloride: formulation and evaluation. Pharmaceutics. 2022 Apr 22;14(5):916. doi: 10.3390/pharmaceutics14050916, PMID 35631501.
29. Rashmitha V, Madhusudan RY, Pavani S. Formulation and evaluation of fenoverine floating tablets. Asian J Pharm Clin Res. 2021 Apr 7;14(4):175-80. doi: 10.22159/ajpcr.2021v14i4.40999.
30. SG, Chandrakala V, Srinivasan S. Development and evaluation of microsponge gel of an antifungal drug. Int J Curr Pharm Sci. 2023 Jan 15;15(1):30-41. doi: 10.22159/ijcpr.2023v15i1.2069.
31. Haju SS, Yadav S. Formulation and evaluation of cilnidipine mucoadhesive buccal film by solvent casting technique for the treatment of hypertension. Int J Pharm Pharm Sci. 2021 Sep 1;13(6):34-43. doi: 10.22159/ijpps.2021v13i9.42641.
32. Loncarevic A, Ivankovic M, Rogina A. Electrosprayed chitosan–copper complex microspheres with uniform size. Materials (Basel). 2021 Sep 28;14(19):5630. doi: 10.3390/ma14195630, PMID 34640029.